

# Development of a 3-D Non-Hydrostatic Pressure Model for Free Surface Flows\*

J. W. Lee    M. D. Teubner    J. B. Nixon<sup>†</sup>    P. M. Gill

September 27, 2004

## Abstract

A three-dimensional non-hydrostatic pressure numerical model for free surface flows is presented. By decomposing the pressure term into hydrostatic and non-hydrostatic parts, the numerical model uses an integrated time step with two fractional steps. In the first fractional step, the momentum equations are solved without the hydrostatic pressure term using Newton's method in conjunction with the generalised minimal residual (GMRES [13]) method. This combined method does not require the determination of a Jacobian matrix explicitly but simply the product of the Jacobian and a vector, thereby reducing the amount of storage required and significantly decreasing the overall computational time required. By using Newton's method, the numerical model can handle implicitly almost all variables, unlike many other numerical models. Hence numerical stability is achieved effectively. In the second fractional step, the pressure-Poisson equation is solved iteratively with a preconditioned linear GMRES. It is shown that pre-conditioning reduces the central processing unit (CPU) time dramatically. After the new pressure field is obtained, the intermediate velocities, which are calculated from the previous fractional step, are updated and then these updated velocities can preserve the local mass conservation. The newly developed model is verified against analytical solutions with good agreement.

---

\*Applied Mathematics, The University of Adelaide, South Australia, AUSTRALIA.  
<mailto:jong.lee@adelaide.edu.au>

<sup>†</sup>United Water International, GPO Box 1875, South Australia, AUSTRALIA.

# Contents

<b>1</b>	<b>Introduction</b>	<b>2</b>
<b>2</b>	<b>Mathematical Formulation</b>	<b>3</b>
<b>3</b>	<b>Numerical Approximation</b>	<b>4</b>
<b>4</b>	<b>Model Validation</b>	<b>6</b>
<b>5</b>	<b>Conclusion</b>	<b>8</b>

## 1 Introduction

Over the past two decades, three-dimensional (3-D) models have been extensively developed and used with the hydrostatic pressure approximation [8, 6]. If the hydrostatic pressure approximation is assumed, the  $z$ -momentum equation is omitted and the vertical velocity is calculated from the continuity equation. Numerical models that use this approximation can be applied to many shallow water flows. However, in some flows in which the ratio of the wave length to the depth is small this approximation is inaccurate. More recently, as computer power has increased dramatically, a few numerical models have been developed that can consider the non-hydrostatic pressure by means of solving a pressure related Poisson equation [3]. The numerical techniques for the pressure-Poisson equation are usually either the semi-implicit method for the pressure-linked equation (SIMPLE)-family methods (SIMPLE [10], SIMPLER [9], SIMPLEC [5]) or fractional time step methods [11]. The SIMPLE methods need multiple iterations per time step until the pressure has converged. Alternatively a fractional time step method can be employed by separating the pressure term into hydrostatic and non-hydrostatic parts and using time marching computations.

In other non-hydrostatic models [2, 7], only parts of the equations are treated implicitly and then the resulting matrix can be inverted inexpensively. For example, the water surface elevation and the vertical diffusion terms in the momentum equations are discretised implicitly in Casulli [2]. In this way, the velocity field is obtained by inverting a tri-diagonal matrix after the water surface elevation is determined. In this study, most terms are solved implicitly using Newton's method with an almost matrix-free methodology. For maximum flexibility in the representation of the computational domain, the governing equations are solved in a generalised coordinate system.

## 2 Mathematical Formulation

In many hydrostatic models [8, 6], it is assumed that the pressure variations depend on the amount of water above a point in vertical space so that it is a function of water surface elevation only, leading to the hydrostatic approximation [14]. However, in this model, the pressure is decomposed into hydrostatic and non-hydrostatic (or hydrodynamic) parts [2] resulting in

$$P = \rho g (h - z) + q, \quad (1)$$

where  $q(x, y, z, t)$  is the non-hydrostatic pressure.

Using the generalised coordinate transformation from  $(x, y, z, t)$  to  $(\xi, \eta, \zeta, \tau)$  with the pressure decomposition, the inviscid 3-D Navier–Stokes equations can be written as

$$\frac{\partial}{\partial \xi} \left( \frac{U}{J} \right) + \frac{\partial}{\partial \eta} \left( \frac{V}{J} \right) + \frac{\partial}{\partial \zeta} \left( \frac{W}{J} \right) = 0, \quad (2)$$

$$\frac{\partial \mathbf{Q}}{\partial \tau} + \frac{\partial \mathbf{E}}{\partial \xi} + \frac{\partial \mathbf{F}}{\partial \eta} + \frac{\partial \mathbf{G}}{\partial \zeta} = \mathbf{P}_h + \mathbf{P}_d, \quad (3)$$

where:  $J = \frac{\partial(\xi, \eta, \zeta)}{\partial(x, y, z)}$  is the Jacobian of the transformation;  $\mathbf{Q}$  represents the unknown variables;  $\mathbf{E}$ ,  $\mathbf{F}$  and  $\mathbf{G}$  are inviscid fluxes in the  $\xi$ –,  $\eta$ – and  $\zeta$ –directions respectively; and  $\mathbf{P}_h$  and  $\mathbf{P}_d$  represent the hydrostatic and non-hydrostatic pressure terms. In matrix form, these variables are defined as:

$$\mathbf{Q} = \frac{1}{J} \begin{pmatrix} u \\ v \\ w \end{pmatrix}, \quad \mathbf{E} = \frac{U}{J} \begin{pmatrix} u \\ v \\ w \end{pmatrix}, \quad \mathbf{F} = \frac{V}{J} \begin{pmatrix} u \\ v \\ w \end{pmatrix}, \quad \mathbf{G} = \frac{W + \zeta_t}{J} \begin{pmatrix} u \\ v \\ w \end{pmatrix}, \quad (4)$$

$$\mathbf{P}_h = -g \begin{pmatrix} \left( \frac{\xi_x}{J} h \right)_\xi + \left( \frac{\eta_x}{J} h \right)_\eta + \left( \frac{\zeta_x}{J} h \right)_\zeta \\ \left( \frac{\xi_y}{J} h \right)_\xi + \left( \frac{\eta_y}{J} h \right)_\eta + \left( \frac{\zeta_y}{J} h \right)_\zeta \\ 0 \end{pmatrix}, \quad (5)$$

$$\mathbf{P}_d = -\frac{1}{\rho} \begin{pmatrix} \left( \frac{\xi_x}{J} q \right)_\xi + \left( \frac{\eta_x}{J} q \right)_\eta + \left( \frac{\zeta_x}{J} q \right)_\zeta \\ \left( \frac{\xi_y}{J} q \right)_\xi + \left( \frac{\eta_y}{J} q \right)_\eta + \left( \frac{\zeta_y}{J} q \right)_\zeta \\ \left( \frac{\xi_z}{J} q \right)_\xi + \left( \frac{\eta_z}{J} q \right)_\eta + \left( \frac{\zeta_z}{J} q \right)_\zeta \end{pmatrix}. \quad (6)$$

$U$ ,  $V$  and  $W$  are the normal velocities at the cell faces (Figure 2), and are determined by

$$\begin{aligned} U &= \xi_x u + \xi_y v + \xi_z w, \\ V &= \eta_x u + \eta_y v + \eta_z w, \\ W &= \zeta_x u + \zeta_y v + \zeta_z w. \end{aligned} \quad (7)$$

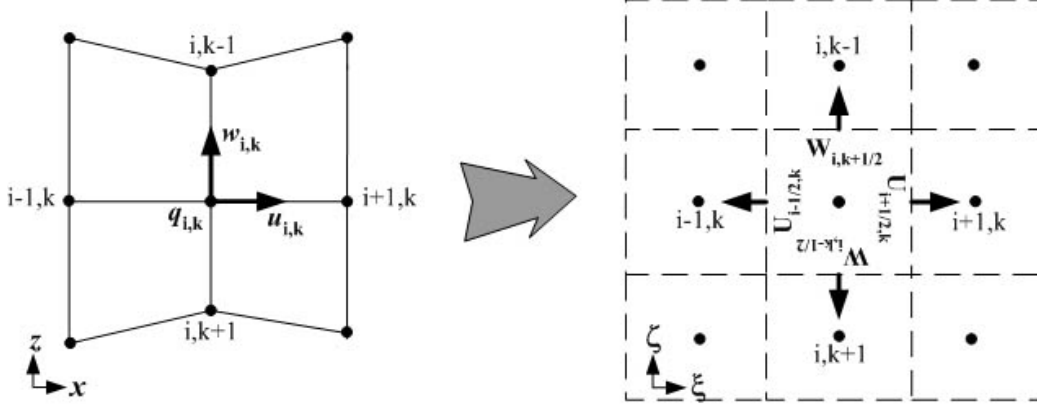


Figure 1: Grid transformation and normal velocities at the cell faces

It should be noted that only the vertical grid changes with time because of the free surface, so that  $\xi_t$  and  $\eta_t$  do not appear in equation (3). In Figure 2, all variables except the normal velocities are defined at the cell centre, resulting in a staggered-like grid scheme. In collocated grids, a checker board pressure field [9] may occur. By locating the normal velocities at the cell faces, however, this can be prevented.

For the free surface, the continuity equation can be integrated from the bottom to the surface leading to:

$$\frac{\partial}{\partial \tau} \left( \frac{h}{J} \right) + \frac{\partial}{\partial \xi} \left( \frac{h\bar{U}}{J} \right) + \frac{\partial}{\partial \eta} \left( \frac{h\bar{V}}{J} \right) = 0, \quad (8)$$

where  $\bar{U} = \xi_x \bar{u} + \xi_y \bar{v}$  and  $\bar{V} = \eta_x \bar{u} + \eta_y \bar{v}$ .

### 3 Numerical Approximation

For the numerical approximation of the inviscid fluxes, the symmetric total variation diminishing (TVD [15]) method is used, wherein rapid changes in the flow fields can be captured using a three-point stencil in one direction. We define the numerical fluxes at cell faces as

$$\mathbf{E}_{i+1/2,j,k}^* = \frac{1}{2} (\mathbf{E}_{i,j,k} + \mathbf{E}_{i+1,j,k}) - \frac{1}{2} U_{i+1/2,j,k} (1 - \phi_{i+1/2,j,k}) \Delta \mathbf{Q}_{i+1/2,j,k} \quad (9)$$

where  $\Delta \mathbf{E}_{i+1/2,j,k} = \mathbf{E}_{i+1,j,k} - \mathbf{E}_{i,j,k}$ , and  $\phi_{i+1/2,j,k}$  is obtained by using the minmod limiter

$$\phi_{i+1/2,j,k} = \min\text{mod}(1, r^+) + \min\text{mod}(1, r^-) - 1, \quad (10)$$

where:

$$r^+ = \frac{\mathbf{Q}_{i-1/2,j,k}}{\mathbf{Q}_{i+1/2,j,k}} \quad \text{and} \quad r^- = \frac{\mathbf{Q}_{i+3/2,j,k}}{\mathbf{Q}_{i+1/2,j,k}}; \quad (11)$$

and the minmod function is defined as

$$\text{minmod}(x, y) = \begin{cases} 0 & \text{for } xy \leq 0, \\ x & \text{for } |x| \leq |y|, \\ y & \text{for } |x| > |y|. \end{cases} \quad (12)$$

Linear interpolation is applied to find  $U$  at cell faces. A similar approximation is applied for the  $\eta$ - and  $\zeta$ -directional fluxes and the depth integrated fluxes in the water surface equation.

For time integration, the governing equations are solved using two fractional time steps involving hydrostatic and non-hydrostatic pressure. For the first hydrostatic step, equation (3) without the non-hydrostatic term is written as:

$$\mathcal{F}(\tilde{\mathbf{Q}}) = \frac{\partial \tilde{\mathbf{Q}}}{\partial \tau} + \frac{\partial \tilde{\mathbf{E}}}{\partial \xi} + \frac{\partial \tilde{\mathbf{F}}}{\partial \eta} + \frac{\partial \tilde{\mathbf{G}}}{\partial \zeta} - \tilde{\mathbf{P}}_{\mathbf{a}} = 0, \quad (13)$$

where  $\mathcal{F}$  is the function representing the momentum equations to be solved and  $\tilde{\mathbf{Q}}$ , etc. denote intermediate solutions which are to be modified in the second step by solving the non-hydrostatic pressure. This equation is solved using the Newton-GMRES method with a matrix-free technique [1].

In the second, non-hydrostatic step, the new velocities are calculated by considering the non-hydrostatic pressure term so that the velocities satisfy the local mass conservation. The non-hydrostatic pressure with the time derivatives of velocities can be written in semi-discrete form as:

$$\begin{aligned} u^{n+1} &= \tilde{u} - \Delta\tau\zeta_t \frac{\partial \tilde{u}}{\partial \zeta} - \frac{\Delta\tau}{\rho} (\xi_x q_\xi + \eta_x q_\eta + \zeta_x q_\zeta)^{n+1}, \\ v^{n+1} &= \tilde{v} - \Delta\tau\zeta_t \frac{\partial \tilde{v}}{\partial \zeta} - \frac{\Delta\tau}{\rho} (\xi_y q_\xi + \eta_y q_\eta + \zeta_y q_\zeta)^{n+1}, \\ w^{n+1} &= \tilde{w} - \Delta\tau\zeta_t \frac{\partial \tilde{w}}{\partial \zeta} - \frac{\Delta\tau}{\rho} (\xi_z q_\xi + \eta_z q_\eta + \zeta_z q_\zeta)^{n+1}. \end{aligned} \quad (14)$$

Substituting equation (14) into the continuity equation (2) gives an elliptic equation, which is called the pressure-Poisson equation. After approximating the second order derivatives of the Poisson equation with the following equations (15a)–(15b), a 19-diagonal matrix is obtained that is solved with a preconditioned linear GMRES. In the current grid system like a staggered grid system, dynamic pressure boundary conditions can be replaced by specifying a normal velocity. For instance,  $U_{-1/2,j,k} = U_{1/2,j,k}$  can be applied to

an impermeable boundary wall ( $i = 1$ ). When the new pressure field is obtained, velocities are updated using equation (14) which will satisfy the local mass conservation, while the global mass conservation can be obtained by solving equation (8).

$$\frac{\partial}{\partial \xi} \left( L \frac{\partial M}{\partial \xi} \right) = \frac{1}{(\Delta \xi)^2} [L_{i+1/2,j,k}(M_{i+1,j,k} - M_{i,j,k}) - L_{i-1/2,j,k}(M_{i,j,k} - M_{i-1,j,k})], \quad (15a)$$

$$\begin{aligned} \frac{\partial}{\partial \xi} \left( L \frac{\partial M}{\partial \eta} \right) = \frac{1}{4\Delta \xi \Delta \eta} [ & L_{i+1/2,j,k}(M_{i+1,j+1,k} - M_{i+1,j-1,k} \\ & + M_{i,j+1,k} - M_{i,j-1,k}) \\ & - L_{i-1/2,j,k}(M_{i,j+1,k} - M_{i,j-1,k} \\ & + M_{i-1,j+1,k} - M_{i-1,j-1,k})]. \end{aligned} \quad (15b)$$

## 4 Model Validation

The newly developed model has been validated by testing a standing wave in a closed basin of square domain (10 m  $\times$  10 m) with inviscid flow approximation. By choosing a relatively small wave length  $\lambda$  compared to the depth  $h_0$ , the hydrostatic approximation is no longer valid. Initially, all velocities are set to zero and the water surface elevation is given by:

$$h(x) = \eta_0 \cos \left( \frac{2\pi}{\lambda} x \right) + h_0 \quad \text{with} \quad 0 \leq x \leq 10, \quad (16)$$

where:  $\eta_0 = 0.1$  m is the amplitude;  $\lambda = 20$  m is the wave length; and  $h_0 = 10$  m is the undisturbed water depth. A zero flow Neumann condition is used for all three velocities at the wall boundaries, while a free slip condition is applied at the free surface. The computational domain uses a constant grid spacing of 0.5 m in the lateral and horizontal directions with 20 layers in the vertical direction. The time step  $\Delta \tau = 0.01$  sec is used for all computations.

Based on small amplitude theory [4], the wave celerity  $c$  is approximated by

$$c = \sqrt{\frac{g\lambda}{2\pi} \tanh \left( \frac{2\pi}{\lambda} h_0 \right)}, \quad (17)$$

which is equivalent to  $c = 3.64$  m/s so that the period  $T$  is 3.59 sec. On the other hand, using the hydrostatic pressure approximation, the wave celerity is given by  $c = \sqrt{gh_0} = 9.90$  m/s and  $T = 2.02$  sec. Therefore the sloshing wave of the hydrostatic model will propagate at a faster speed than that of the non-hydrostatic model.

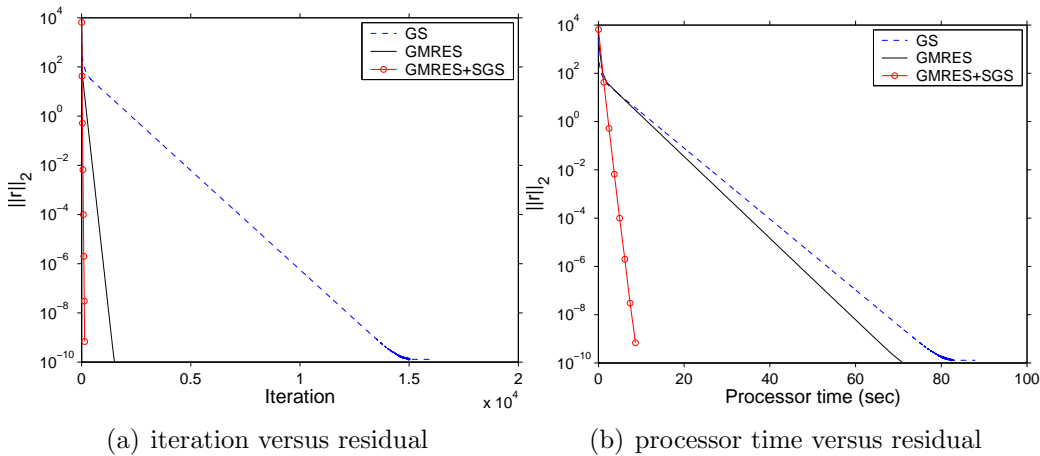


Figure 2: Convergence test for three iterative methods

Let us examine the convergence rate of the Poisson equation using three iterative methods: the Gauss–Seidel (GS) method and the GMRES with and without SGS pre-conditioning [12]. In Figure 4, the  $y$ –axis represents the Euclidean norm of the residual plotted against the number of iterations in Figure 2(a) and the processor time in sec in Figure 2(b). In these figures, the residual  $r = b - Ax^{(m)}$  where  $b$  is the right hand side of the linear system,  $A$  is the Jacobian and  $x^{(m)}$  is the estimation of pressure at the  $m^{\text{th}}$  iteration. As expected, the Gauss–Seidel method converges most slowly and cannot reduce the residual norm below  $10^{-10}$ . The GMRES without pre-conditioning is an improvement over the Gauss–Seidel method. However, when it is used with the SGS, the number of iterations is reduced dramatically. Even though extra calculations are needed for the pre-conditioning matrix, the overall performance is the best using GMRES with SGS.

Figure 4 shows the calculated velocity fields, with and without the hydrostatic pressure approximation, at  $y = 5$  m at time  $t = T/4$ , which is equivalent to 0.505 sec and 0.898 sec, respectively. The most significant difference is that the hydrostatic model calculates much larger vertical velocities near the walls than the non-hydrostatic model. This is because, with the hydrostatic approximation, these velocities are calculated by solving the continuity equation so that they are only a function of the horizontal velocity field. The results from the hydrostatic model suggest that velocity variations over depth, especially near  $x = 5$  m, are almost negligible; this is consistent with the shallow water approximation.

The computed velocity and hydrodynamic pressure fields are compared

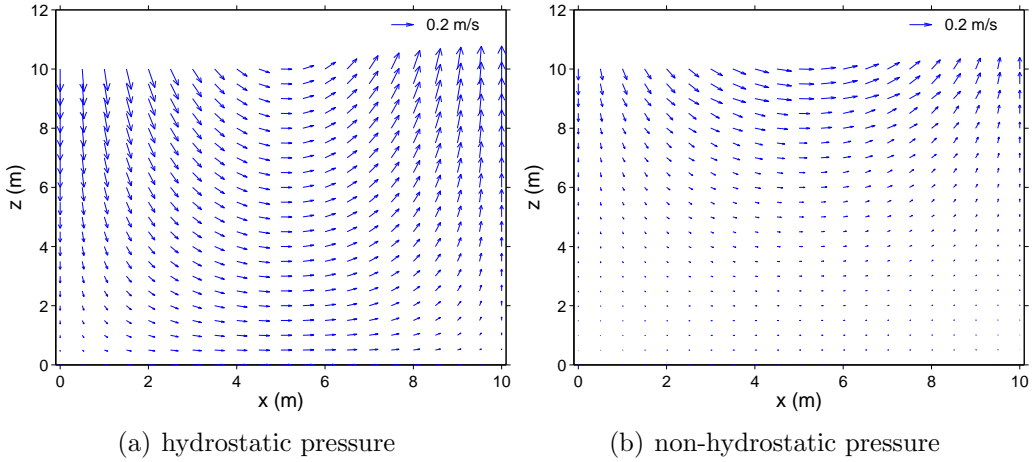


Figure 3: Velocity vector plots, with and without the hydrostatic pressure approximation, at time  $t = T/4$

with the analytical solutions [4] at time  $t = T/8$  in Figure 4. At this time, the water surface is dropping to the equilibrium position on the left and rising on the right; negative pressure is shown on the left hand side. Excellent agreement between these results indicates that the normal velocity boundary condition has been applied to the pressure-Poisson equation correctly.

## 5 Conclusion

In this paper, a 3-D numerical model with and without the hydrostatic approximation is presented using a generalised coordinate system. Time integration is performed using two fractional time steps. In the hydrostatic fractional step, the intermediate velocity field is solved using a Newton–GMRES method. By considering the non-hydrostatic pressure and the continuity equation, the intermediate velocities are updated to the divergence free velocities in the non-hydrostatic step. In the second fractional step, the pressure-Poisson equation is solved using the GMRES with SGS preconditioning. The newly developed model has been tested with an idealised case and compared with analytical solutions. Overall agreement with the analytical solutions verifies the accuracy of the current numerical model.

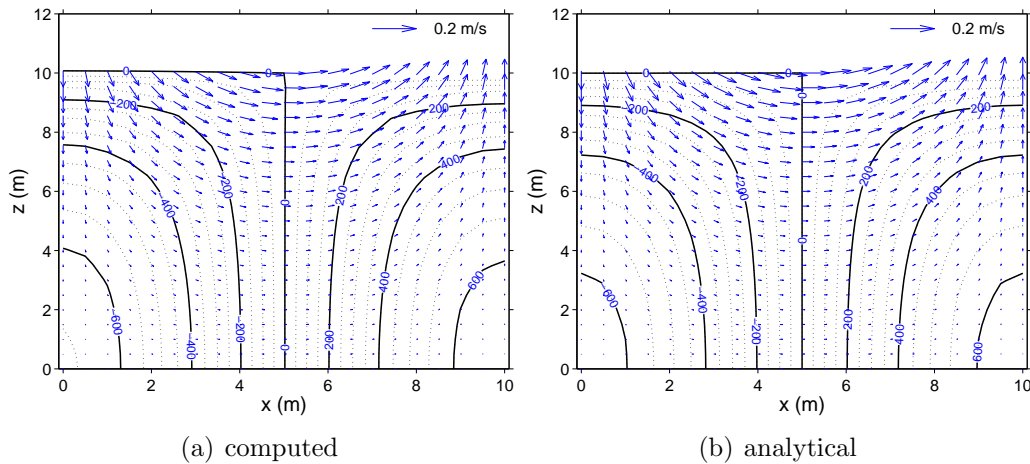


Figure 4: Velocity and hydrodynamic pressure fields, as computed by the model and as determined analytically

## References

- [1] P. N. Brown and Y. Saad. Hybrid Krylov methods for nonlinear systems of equations. *SIAM J. Sci. Stat. Comput.* 1990, **11**:450–481.
- [2] V. Casulli. A semi-implicit finite difference method for non-hydrostatic, free-surface flows. *Int. J. Numer. Meth. Fluids* 1999, **30**:425–440.
- [3] V. Casulli and E. Cattani. Stability, accuracy and efficiency of a semi-implicit method for three-dimensional shallow water flow. *Comp. and Maths with Applications* 1994, **27**:99–112.
- [4] R. G. Dean and R. A. Dalrymple. *Water Wave Mechanics for Engineers and Scientists*. World Scientific, 1991.
- [5] J. P. van Doormaal and G. D. Raithby. Enhancements of the SIMPLE method for predicting incompressible fluid flows. *Numer. Heat Transfer* 1984, **7**:147–163.
- [6] W. Huang and M. Spaulding. 3D model of estuarine circulation and water quality induced by surface discharges. *J. Hydraul. Eng.* 1995, **121**:300–311.
- [7] M. B. Koçyigit, R. A. Falconer and B. Lin. Three-dimensional numerical modelling of free surface flows with non-hydrostatic pressure. *Int. J. Numer. Meth. Fluids* 2002, **40**:1145–1162.

- [8] Q. Lu and O. W. H. Wai. An efficient operator splitting scheme for three-dimensional hydrodynamic computations. *Int. J. Numer. Meth. Fluids* 1998, **26**:771–789.
- [9] S.V. Patankar. *Numerical Heat Transfer and Fluid Flow*. McGraw Hill, 1980.
- [10] S. V. Patankar and D. B. Spalding. A calculation procedure for heat, mass and momentum transfer in three-dimensional parabolic flows. *Int. J. Heat Mass Transfer* 1972, **15**:1787–1806.
- [11] C. M. Rhie and W. L. Chow. Numerical study of the turbulent flow past an airfoil with trailing edge separation. *AIAA Journal* 1983, **21**:1525–1532.
- [12] Y. Saad. *Numerical Methods for Large Eigenvalue Problems (Algorithms and Architectures for Advanced Scientific Computing)*. John Wiley and Sons Inc, 1992.
- [13] Y. Saad and M. H. Schultz. GMRES: A generalized minimal residual algorithm for solving nonsymmetric linear systems. *SIAM J. Sci. Stat. Comput.* 1986, **7**:856–869.
- [14] C. B. Vreugdenhil. *Numerical Methods for Shallow-Water Flow*. Kluwer Academic Publishers, 1994.
- [15] H. C. Yee. Construction of explicit and implicit symmetric TVD schemes and their applications. *J. Comput. Physics* 1987, **68**:151–179.